Eur. Phys. J. Spec. Top. (2026) 235:8425–8434
https://doi.org/10.1140/epjs/s11734-026-02527-0

THE EUROPEAN PHYSICAL JOURNAL SPECIAL TOPICS

Regular Article

Brain network dynamics during evidence accumulation in memory task: evidence from fNIRS and drift–diffusion model

Artem Badarin[1,4,a], Vladimir Antipov[1,4], Susanna Gordleeva[5], and Vladimir Maksimenko[1,2,3]

[1] Plekhanov Russian University of Economics, 36 Stremyanny Lane, Moscow, Russia
[2] Neimark University, 6 Nartova St., Nizhniy Novgorod, Russia
[3] Innopolis University, 1 Universitetskaya St., Innopolis, Russia
[4] National Medical Research Center for Therapy and Preventive Medicine, 10 Petroverigskiy Pereulok, Moscow, Russia
[5] Lobachevsky State University of Nizhny Novgorod, 23 Prospekt Gagarina (Gagarin Avenue), Nizhniy Novgorod, Russia

Received 25 May 2026 / Accepted 7 July 2026 / Published online 17 July 2026
© The Author(s), under exclusive licence to EDP Sciences, Springer-Verlag GmbH Germany, part of Springer Nature 2026

Abstract Understanding the neural mechanisms underlying different stages of memory processing remains a challenge in cognitive neuroscience. The Drift Diffusion Model (DDM) provides an effective framework to dissociate these processes by linking memory extraction to non-decision time and evidence comparison to drift rate. In the present study, we investigate this possibility using brain network activity recorded with functional near-infrared spectroscopy during a memory scanning task. We hypothesize that neuronal network properties reflect higher-level cognitive processes involved in stimulus interpretation and evidence accumulation, rather than more basic processes related to memory extraction. To test this, we estimate DDM parameters and relate them to graph-theoretical measures of brain networks, including mean coupling strength and clustering coefficient. Our results demonstrate that network properties are selectively associated with drift rate, but not with non-decision time. Specifically, higher coupling strength is associated with lower drift rates, suggesting increased demands on information processing and slower evidence accumulation. In contrast, higher clustering coefficients are associated with higher drift rates, indicating more efficient local processing during decision formation. These findings suggest that large-scale network organization primarily supports higher-order cognitive processes involved in evidence accumulation, rather than early-stage memory retrieval, providing new insights into the neural basis of decision-making in memory tasks.

1 Introduction

In cognitive psychology, experiments typically involve presenting stimuli to participants and collecting their behavioral responses, such as response times and accuracy. These measures are then used to infer how cognitive processing differs across conditions and between groups. However, behavioral data provide only limited insight into underlying cognitive processes. Even simple tasks, such as perceptual decision-making tasks, involve multiple components, including stimulus encoding, evidence accumulation, decision formation, and motor response execution. Consequently, observed behavioral effects, such as increased response time or reduced accuracy, may arise from changes in different processing stages. For example, longer response times may reflect slower sensory encoding, increased motor preparation time, or prolonged evidence accumulation [1, 2].

Therefore, it is important to dissociate stimulus processing into its constituent components to gain deeper insights into cognitive mechanisms. This is particularly relevant for memory tasks, which, in addition to processing visual information, require retrieval of stored information. In such tasks, an additional critical stage involves extracting relevant information from memory, which is essential for successful performance in memory scanning paradigms. To address this complexity, computational frameworks are used to decompose behavior into distinct components. One such framework is the Drift Diffusion Model (DDM), which separates decision-making into evidence accumulation (drift rate) and non-decision processes (e.g., encoding and motor response). In memory scanning tasks, this model

[a] e-mail: badarin.a.a@mail.ru (corresponding author)

allows linking memory retrieval processes to non-decision time, while the utilization of retrieved information for stimulus interpretation is reflected in the drift rate [3, 4]. This dissociation opens the possibility of identifying neural correlates of these components. Earlier work in this area has demonstrated associations between DDM components and local measures of brain activity, such as event-related potentials and band-specific power of neural signals [3, 5, 6]. At the same time, the relationship between DDM components and properties of functional brain networks remain largely unexplored.

Over the past decade, graph-theoretical analysis of functional brain networks has emerged as a powerful framework to characterize large-scale neural organization [7–10]. Functional connectivity, estimated from neuroimaging data such as functional near-infrared spectroscopy (fNIRS) or fMRI, can be represented as a graph where nodes correspond to recording channels or brain regions and edges represent statistical dependencies between their time series [7, 11]. Measures such as mean connectivity (global coupling strength) and clustering coefficient (local segregation) have been successfully used to quantify task-related reorganization of cortical networks [12–14]. For instance, network approaches have been applied to study cognitive load, attention, and working memory [15, 16], as well as to analyze publication trends in AI medical applications [17]. Moreover, recent methodological advances combining fNIRS with network analysis have enabled the classification of motor-related brain activity [18] and the development of neuroadaptive systems for enhancing cognitive abilities [19]. In parallel, the use of Riemannian geometry to analyze eye-movement covariance matrices during working memory tasks has further highlighted the rich information embedded in multi-dimensional behavioral and neural data [20]. However, despite this progress, no study to date has directly linked DDM parameters—particularly drift rate and non-decision time—to graph-theoretic properties of brain networks reconstructed from fNIRS data in a memory scanning task.

In the present study, we hypothesize that functional brain network properties, such as integration and clustering, are associated with higher-level cognitive processes involved in evidence accumulation, rather than basic memory extraction [15, 16]. Specifically, among DDM parameters, we expect network measures to be associated with drift rate, but not with non-decision time. This hypothesis is grounded in the idea that large-scale cortical coordination becomes relevant when retrieved information is compared with the probe and a decision is formed, whereas memory retrieval itself may rely on more local or subcortical mechanisms [21]. Testing this hypothesis is particularly novel because previous studies have either focused on local neural correlates of DDM components (e.g., EEG oscillations) or examined network properties only in relation to raw behavioral performance (response times or accuracy), without decomposing the decision process into its latent constituents. By combining trial-wise fNISS-based network reconstruction with hierarchical Bayesian drift–diffusion modeling, we provide the first evidence that global network integration and local clustering selectively modulate evidence accumulation efficiency, while leaving non-decision processes unaffected.

To test these hypotheses, we conduct a memory scanning experiment in which participants encode a set of stimuli, retain it in memory, and subsequently respond to a probe indicating whether it was part of the set. Brain activity is recorded using fNIRS, and functional connectivity between brain regions is estimated based on oxygenation responses. From these data, we compute graph-theoretical measures, including mean network strength (reflecting integration) and clustering coefficient (reflecting local processing). Our results show that network measures are associated with drift rate, but not with non-decision time. Specifically, higher network integration is associated with lower drift rates, suggesting increased processing demands and reduced efficiency of evidence accumulation. In contrast, higher clustering coefficients are associated with higher drift rates, indicating more efficient local processing. These findings suggest that brain network organization primarily supports higher-order cognitive processes involved in evidence accumulation rather than memory extraction, and they open new avenues for using DDM-driven network analysis in cognitive and clinical neuroscience [22–24].

2 Methods

2.1 Participants

A total of fourteen healthy volunteers (9 men and 5 women), aged between 18 and 22 years, took part in the study. All participants had normal or corrected-to-normal vision. Prior to the experiment, each volunteer was given a detailed explanation of the task, had the opportunity to clarify any questions regarding the procedure, and signed a written informed consent form. The study was conducted in accordance with the principles of the Declaration of Helsinki, and the experimental protocol was approved by the local Research Ethics Committee of Innopolis University.

2.2 Experimental procedure

Participants performed a Sternberg-type memory scanning task [25–27]. Visual stimuli were presented on a 24-inch monitor with a resolution of 1920 × 1080 pixels and a refresh rate of 60 Hz. The viewing distance was approximately 0.8 m. Responses were given using a joystick.

Each trial consisted of five successive stages (Fig. 1a). First, a fixation cross was presented for 1.5–2.5 s. Second, a memory set of letters was displayed for 1.5–2.5 s. The number of letters in the presented memory set was defined as the set size. In the present study, set size varied from 2 to 7 letters, thereby manipulating memory load. Third, a retention interval of 3–7 s followed, during which participants maintained the encoded letters in working memory. Fourth, a single probe letter was presented for 2 s. Participants were required to determine whether the probe had been included in the preceding memory set. Finally, a 2-s interval was provided for response execution.

Thus, the task structure included attentional orienting, encoding of the memory set, short-term retention, probe-based comparison with the stored representation, and response execution. This sequential organization was suitable for the subsequent drift–diffusion analysis, as probe evaluation was assumed to reflect evidence accumulation, whereas encoding and response-related processes contributed primarily to non-decision components.

Both target-present and target-absent trials were included across all set sizes, and trial order was randomized. Each participant was presented with 288 trials, organized into four blocks of 72 trials each. Within every block, each of the six set sizes (2–7 letters) was presented 12 times, yielding 48 trials per set size. Within each set-size condition, target-present and target-absent trials were balanced. Response time was defined as the interval between probe onset and the behavioral response.

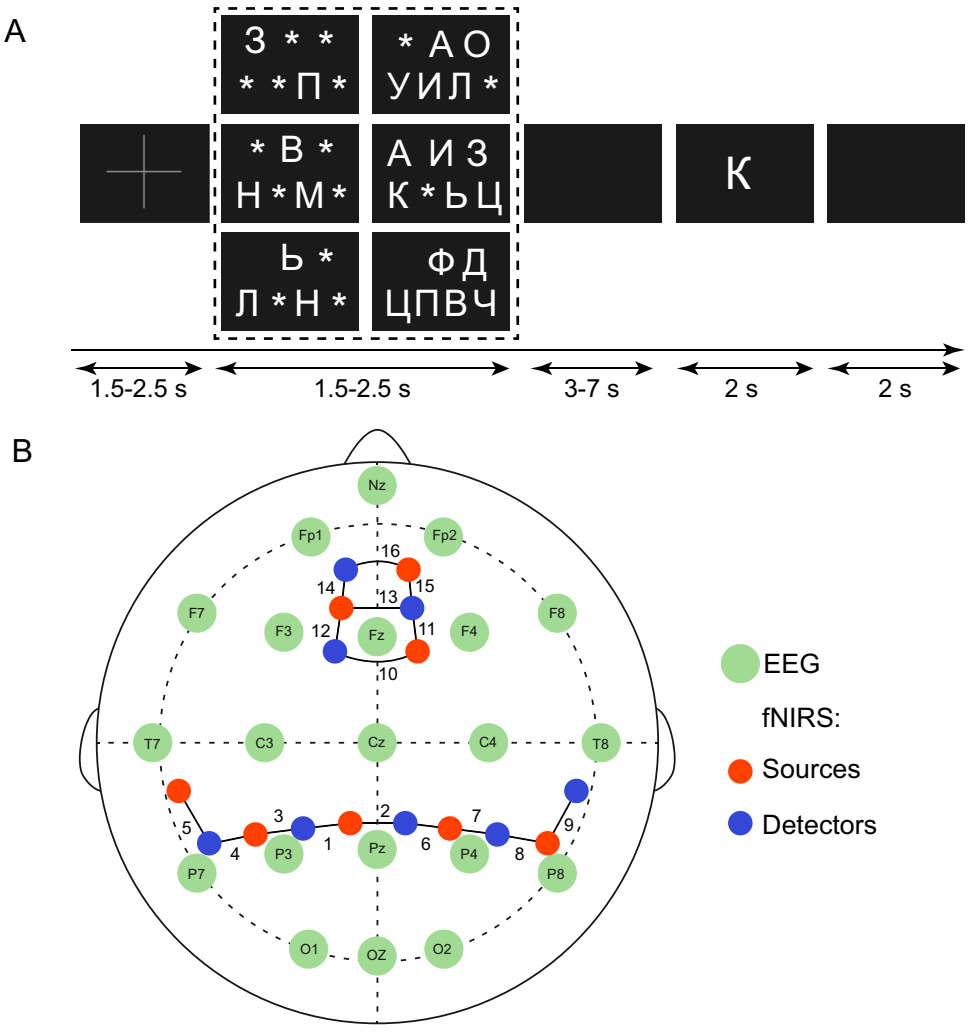


Fig. 1 Experimental paradigm and sensor arrangement. **A** Schematic illustration of the Sternberg-type memory scanning task. Each trial included fixation, memory-set presentation, retention, probe evaluation, and response. Memory load was manipulated by varying the set size from 2 to 7 letters. **B** Arrangement of fNIRS optodes over frontoparietal regions. Green circles indicate EEG electrode positions shown for anatomical reference only, red circles denote fNIRS sources, and blue circles denote fNIRS detectors

2.3 fNIRS recording and network analysis

Hemodynamic activity was recorded from frontoparietal cortical regions using functional near-infrared spectroscopy. Signals were acquired with a NIRScout system manufactured by NIRx Medizintechnik GmbH (Berlin, Germany). The NIRScout is a continuous-wave multichannel fNIRS device that emits near-infrared light at two wavelengths (760 and 850 nm), enabling simultaneous monitoring of changes in oxygenated and deoxygenated hemoglobin concentrations in cortical tissue. The recording montage comprised 16 channels formed by source–detector pairs distributed over the bilateral frontal and parietal cortex (Fig. 1b), and the optical intensities were sampled at $F_s = 7.8125$ Hz.

2.3.1 NIRS preprocessing

For each channel of the optode montage, the raw optical intensity signals were converted into time series of oxygenated hemoglobin (HbO) concentration changes using the modified Beer–Lambert law [28]. All subsequent analyses were performed on the HbO signals, which provide the most informative index of task-related cortical activation in fNIRS and exhibit strong correspondence with the BOLD response measured by fMRI [29].

To isolate the neurovascular component of the signal, each channel was band-pass filtered in the range 0.01–0.2 Hz using a fourth-order zero-phase Butterworth IIR filter. The lower cutoff was chosen to attenuate slow baseline drifts of instrumental and physiological origin, while the upper cutoff was set to suppress cardiac pulsations and high-frequency measurement noise. The retained pass-band preserves the neurovascular oscillations together with the slower systemic fluctuations that are relevant for the cognitive task under study.

The filtered signals were subsequently segmented into single-trial windows. Each window covered the full sequence of task-related events, starting from the onset of the memory-set presentation and extending through the retention interval, probe evaluation, and response execution, up to the onset of the next fixation cross (approximately 4 s after probe offset). In addition to the trial windows, a baseline reference interval was extracted from the period between the first and the second memory-set presentations at the very beginning of the recording session, prior to active task performance. This reference interval was used in the subsequent normalization step to account for inter-individual differences in baseline functional coupling arising from systemic physiology such as respiration, blood pressure variations, and resting cortical activity.

2.3.2 Brain network reconstruction

Functional brain networks were reconstructed separately for each trial from the preprocessed HbO time series. For each trial window, Pearson correlation coefficients r_{ij} were computed between all distinct channel pairs. To bring correlation values to a scale with approximately normal sampling variance, r_{ij} were Fisher-transformed [30], $z_{ij} = \operatorname{arctanh}(r_{ij})$, with $|r_{ij}|$ clipped at $1 - \varepsilon$ ($\varepsilon = 10^{-6}$) to avoid divergences. The same procedure was applied to a baseline reference, yielding z_{ij}^{bg}.

The trial network was then represented as a weighted undirected graph with $N = 16$ nodes (fNIRS channels) and edge weights $w_{ij} = |z_{ij} - z_{ij}^{\mathrm{bg}}|$. Baseline subtraction suppresses systematic between-subject differences in functional connectivity arising from non-task-related systemic physiology, while the absolute value ensures symmetric treatment of positive and negative trial-related modulations of functional coupling. The sign of the baseline-corrected connectivity reflects only whether trial-related coupling increased or decreased relative to baseline, whereas its magnitude reflects the strength of the task-related reorganization. As the present network measures quantify the overall extent of coupling change rather than its direction, and averaging signed changes could cause artifactual cancellation and underestimate the true coupling strength, absolute values were used. No thresholding or binarization was applied; all graph-theoretical measures were computed on the fully weighted network.

For each trial, two complementary network measures were extracted. The first is the mean connectivity $\bar{W}$, defined as the average edge weight across all channel pairs, which serves as a global descriptor of coupling strength and reflects the extent of large-scale frontoparietal integration. The second is the global weighted clustering coefficient, computed following Onnela et al. [31]. For each node u, the local clustering is defined as

$$C_u^w = \frac{1}{k_u(k_u - 1)} \sum_{j,k=1}^{N} (\hat{w}_{uj}\, \hat{w}_{uk}\, \hat{w}_{jk})^{1/3}, \tag{1}$$

where $\hat{w}_{ij} = w_{ij} / \max_{kl} w_{kl}$, and k_u is the number of edges incident to node u ($k_u = N - 1$ in the absence of thresholding). The global clustering coefficient $\bar{C}$ is obtained by averaging C_u^w over all nodes. While $\bar{W}$ characterizes large-scale functional integration, $\bar{C}$ quantifies local segregation: high values of $\bar{C}$ indicate that the neighbors of a given channel tend to be strongly coupled to each other [7, 11].

The trial-wise values of $\bar{W}$ and $\bar{C}$ entered the subsequent drift–diffusion analysis relating frontoparietal network organization to behavioral performance and to parameters of the decision process.

2.4 Drift diffusion model

The DDM suggests that decision-making is a noisy competitive evidence accumulation process, which initiates at starting point and evolves over time according to the drift rate with mean and between-trial noise that results in the distribution of response times across trials (see Fig. 2).

The decision is reached when the accumulated evidence first reaches the decision boundary associated with a correct or incorrect option. If the response is correct, evidence reaches upper boundary first at the time moment where response time is a sum of decision time and the non-decision time that encompasses information processing, motor response formation and in memory task retrieving information from the memory. The model parameters including drift rate, its variance, starting point, decision boundary, and non-decision time are estimated when fitting model to the data (response times and correctness) collected in human experiment.

Behavioral data were analyzed using hierarchical Bayesian drift–diffusion modeling implemented in the HDDM package in Python. Trials with missing values were removed, and response times outside the range between 0.2 s and 4 s were excluded following [21]. Continuous predictors, including set size, functional connectivity (mean network strength), and clustering coefficient were standardized (z-scored) prior to model estimation.

We specified a hierarchical regression model in which trial-wise predictors modulated both drift rate (v) and non-decision time (t). Specifically, drift rate and non-decision time were modeled as linear functions of set size, connectivity, and clustering. Boundary separation, drift rate variability, and non-decision time variability were also estimated to capture between-trial variability in decision processes. To handle outliers, we set a corresponding parameter p_{outlier} to 0.05. Model parameters were estimated using Markov Chain Monte Carlo (MCMC) sampling. Starting values were initialized using the built-in optimization procedure, followed by 5000 posterior samples, with the first 1000 samples discarded as burn-in. Posterior traces were stored for subsequent analysis. Convergence of the MCMC simulations was assessed using the potential scale reduction factor $\hat{R}$. All estimated parameters exhibited $\hat{R}$ values below 1.05, indicating satisfactory convergence of the chains and reliable estimation of the posterior distributions.

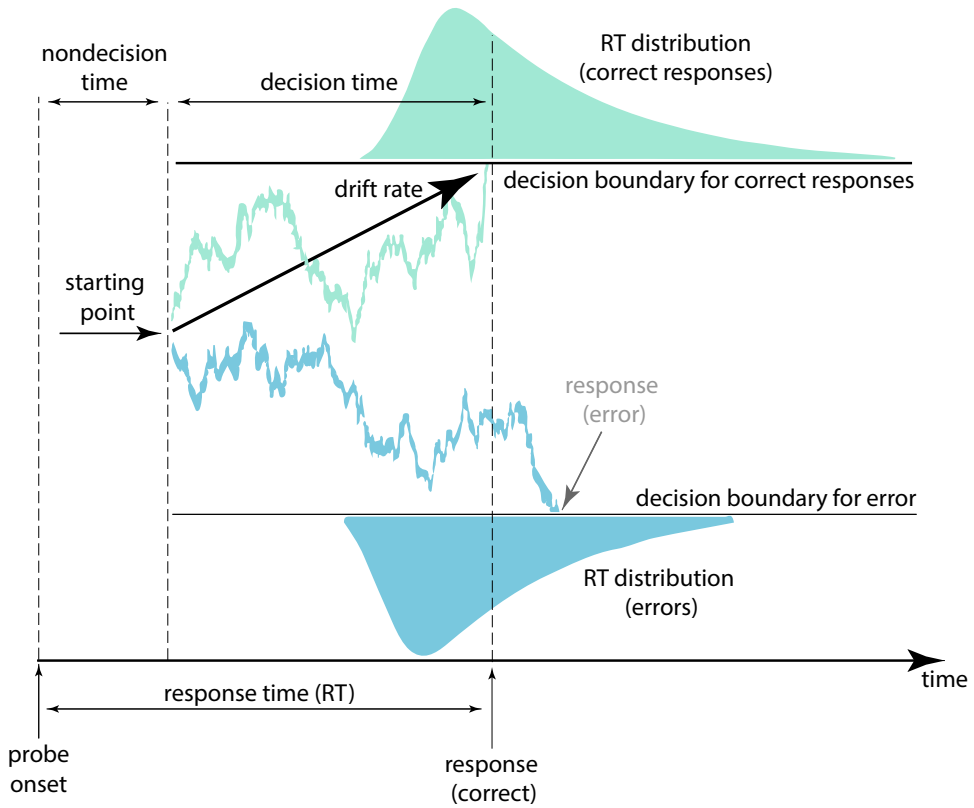


Fig. 2 Illustration of the different DDM parameters. Decision-making in the DDM is modeled as a noisy evidence accumulation process. The accumulation process starts at the starting point and evolves according to the drift rate. Across trials, the drift rate may vary according to a Wiener process with standard deviation σ. A decision is made when the accumulated evidence first reaches the decision boundary associated with one of the response options. In a choice task with one correct option, one boundary corresponds to the correct response, whereas the other corresponds to an error

2.5 Linear mixed-effects modeling of reaction time

To complement the drift–diffusion analysis and examine whether brain network properties were directly associated with response time, we fitted linear mixed-effects models [32] with log-transformed response time (ln(RT)) as the dependent variable. Log transformation was applied to reduce the positive skewness of the response time distribution, as commonly recommended for response latency data [33]. The model included set size, mean connectivity $\bar{W}$, and clustering coefficient $\bar{C}$ as fixed effects, and a subject-specific random intercept to account for repeated measurements within participants. All continuous predictors were standardized (z-scored) prior to fitting, so that the reported fixed-effect estimates correspond to standardized regression coefficients β. Models were estimated using restricted maximum likelihood (REML) with the Powell optimization method, as implemented in the `statsmodels` library in Python. Statistical significance of fixed effects was assessed using Wald z-tests, with effects considered significant at $p < 0.05$. The same modeling framework was applied in control analyses examining whether the network measures themselves varied with set size, with $\bar{W}$ or $\bar{C}$ as the dependent variable.

3 Results

In the memory scanning task, observed response time was strongly associated with memory set size, such that larger set sizes led to longer response times ($\beta \approx 0.20$, $p < 0.001$). In contrast, after controlling for set size, there were no significant associations between response time and network properties. Both connectivity ($\beta \approx 0.03$, $p > 0.3$) and clustering ($\beta \approx 0.02$, $p > 0.4$) showed non-significant effects. Similarly, choice set size was not meaningfully related to network properties. Neither connectivity ($\beta \approx -0.02$, $p > 0.3$) nor clustering ($\beta \approx 0.00$, $p > 0.9$) showed significant associations with set size.

In contrast, analysis of the associations between DDM parameters, set size, and network properties revealed meaningful associations (see Fig. 3).

For the drift rate (Fig. 3, top row), all three predictors showed systematic effects. Increasing set size was associated with a substantial decrease in drift rate, as the entire credible interval lay below zero, indicating slower evidence accumulation under higher task demands. Functional connectivity also showed a negative effect on the drift rate, with credible intervals largely below zero, suggesting that higher global network integration is associated with less efficient evidence accumulation. In contrast, the clustering coefficient exhibits a positive effect on drift rate, with credible intervals above zero, indicating that greater local network organization supports faster evidence accumulation.

For non-decision time (Fig. 3, bottom row), the pattern differed. Set size showed a clear positive effect, with credible intervals entirely above zero, indicating longer non-decision processes for larger choice sets. In contrast, both connectivity and clustering effects on non-decision time are centered around zero, with credible intervals overlapping zero, suggesting no reliable association.

Overall, these results demonstrate a dissociation between cognitive components: network properties selectively relate to evidence accumulation (drift rate), but not to non-decision processes, whereas task difficulty (set size) affects both components.

A further inspection of Fig. 3 highlights that, although all three predictors contributed to drift rate, their effects differed in sign and in relative magnitude. The effect of set size was by far the most pronounced, with the posterior distribution shifted clearly into the negative range and the entire 95% credible interval well below zero, reflecting a consistent slowing of evidence accumulation under higher memory load. The effects of the two network measures were smaller in magnitude, with their 90% credible intervals lying entirely on a single side of zero, and crucially pointed in opposite directions: mean coupling strength contributed negatively, whereas the clustering coefficient contributed positively to drift rate. This pattern indicates that the two network descriptors capture complementary, rather than redundant, aspects of frontoparietal organization during the task, with large-scale integration and local segregation exerting opposing influences on the efficiency of evidence accumulation. In contrast, for non-decision time, only the effect of set size was clearly non-zero, while the posterior distributions for both network measures straddled zero. Together, these observations support a selective coupling between network organization and the decision component of the task, while pre- and post-decisional processes appear to be primarily modulated by task difficulty.

4 Discussion

The present study examined how functional brain network organization relates to distinct cognitive components of memory-based decision-making, as captured by the drift–diffusion model. Three main findings emerged: memory set size produced reliable effects on both DDM parameters, decreasing drift rate and increasing non-decision time;

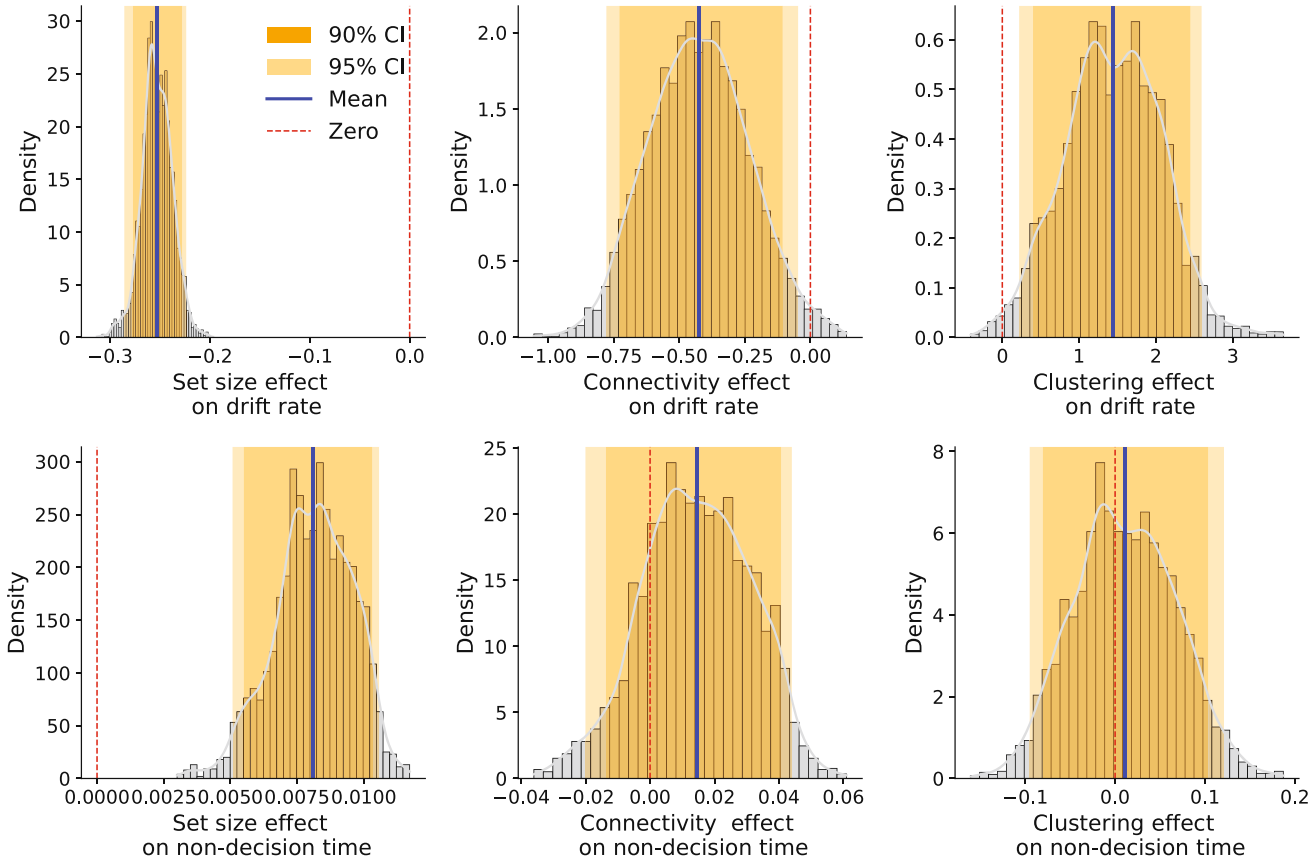


Fig. 3 Posterior distributions of drift–diffusion model parameters. Histograms with kernel density approximations show the posterior distributions of regression coefficients linking choice set size, connectivity measure and clustering coefficients to DDM parameters. The top row presents effects on drift rate (evidence accumulation), and the bottom row presents effects on non-decision time. Panels correspond to set size, functional connectivity (mean network strength), and clustering coefficient. Shaded regions indicate the 95% (light orange) and 90% (dark orange) credible intervals, the blue vertical line denotes the posterior mean, and the red dashed line marks zero effect. Parameters whose credible intervals do not overlap zero indicate reliable associations with the corresponding DDM parameter

frontoparietal network properties were selectively associated with drift rate, but not with non-decision time; and higher mean coupling strength predicted lower drift rates, whereas higher clustering coefficients predicted higher drift rates.

The joint effect of set size on drift rate and non-decision time is consistent with a growing literature applying diffusion-model analyses to working-memory tasks. Shepherdson, Oberauer, and Souza [21] reported that, across several variants of a local recognition task, increasing memory load systematically decreased drift rate and increased non-decision time, and interpreted these effects within a two-stage model in which retrieval and decision are at least partially non-overlapping: the time needed to bring the relevant representation into the focus of attention is reflected in non-decision time, whereas the quality of the retrieved representation governs drift rate. Our results reproduce this dissociation in a Sternberg-type memory scanning task, supporting the generality of the two-stage account.

A central result of the present work is that trial-wise frontoparietal network measures were systematically associated with drift rate, but not with non-decision time. This suggests that large-scale fNIRS connectivity primarily reflects higher-order cognitive processes related to stimulus interpretation and evidence accumulation, rather than the more non-decisional stages of sensory encoding, motor preparation, or memory retrieval. The two stages may, therefore, be supported by distinct neural mechanisms, with retrieval-related processes operating at a more local or subcortical level, while large-scale cortical coordination becomes relevant when the retrieved information is compared with the probe and a decision is formed. It should be noted that non-decision time is itself a composite quantity, combining stimulus encoding, memory retrieval, and motor processes rather than reflecting memory retrieval alone. Accordingly, the absence of an association between network measures and non-decision time concerns this composite component, and not memory retrieval specifically.

The opposite signs of the two network effects on drift rate further clarify the functional meaning of these measures. Higher mean coupling strength was associated with lower drift rates, plausibly reflecting increased processing demands and the recruitment of additional neural resources, consistent with previous work linking task difficulty and cognitive load to increased global integration [15]. In contrast, higher clustering coefficients were associated with higher drift rates, suggesting that a more modular, locally organized network configuration supports more efficient evidence accumulation. A conceptually related pattern was reported in [34], who showed that more structured (lower-entropy) scanpaths during encoding predicted better subsequent memory performance. Although the modality and scale differ, the underlying principle is similar: organized, locally structured processing supports performance, whereas more diffuse processing is associated with reduced efficiency.

Notably, raw response times in our experiment did not show significant associations with the network measures, although these measures were reliably related to drift rate in the DDM analysis. Response time is a composite measure that integrates encoding, retrieval, evidence accumulation, and motor execution, so that effects on a specific component can be masked at the behavioral level by variability in the others. The DDM decomposes response time into latent components and thereby provides a more sensitive window onto the cognitive processes most strongly linked to network organization, in line with previous DDM-based analyses of working memory [21].

These results fit into a broader picture in which memory-based decision-making is supported by distributed mechanisms operating on multiple scales, from local oscillatory signatures of evidence accumulation [3, 5, 6] to oculomotor signals linked to working-memory retrieval [35]. The present work complements this picture by showing that large-scale cortical network organization is most informative about the evidence accumulation stage of the decision. Several limitations should nonetheless be acknowledged: fNIRS is sensitive only to superficial cortical signals, network measures were computed over the entire trial interval rather than separately for encoding, retention, and probe evaluation, and the sample is relatively small. The modest sample size ($N = 14$) limits the generalizability of the present findings and reduces statistical power for detecting small effects. This limitation is partially mitigated by the hierarchical Bayesian formulation, which pools information across participants and relies on trial-wise predictors; nevertheless, replication in larger and more diverse samples is required. Future studies combining fNIRS with EEG and eye-tracking, and employing time-resolved connectivity analyses, would help to refine the mapping between network organization and the cognitive components of memory-based decisions.

5 Conclusions

Our results demonstrate a clear dissociation between task demands and brain network organization in memory-based decision processes. Increasing choice set size consistently impairs performance by reducing drift rate and increasing non-decision time. These results are aligned with literature suggesting that increasing set size increases time to extract information from memory and then slows down evidence accumulation rate. In contrast, functional network properties selectively relate to evidence accumulation: higher global connectivity is associated with reduced drift rates, that may suggest increased processing demands and higher cognitive load, whereas higher clustering is associated with enhanced drift rates, probably reflecting local information processing which is computationally more efficient. Importantly, these network measures do not influence non-decision time, indicating that they are specifically linked to higher-order cognitive operations related to stimulus interpretation and decision making rather than more low-level processes such as extraction from memory, sensory encoding or motor execution.

Note that, registered response times did not show significant associations with network measures, whereas these measures were related to drift rate in the drift–diffusion model. This dissociation likely reflects the fact that response time represents a composite measure that combines multiple processing stages, including both evidence accumulation and non-decision processes. As a result, effects on specific cognitive components, such as evidence accumulation efficiency, may be obscured at the behavioral level. In contrast, the drift–diffusion model decomposes response time into latent components, allowing selective identification of relationships between neural network properties and evidence accumulation (drift rate). This suggests that network organization primarily modulates the efficiency of information processing rather than overall response speed.

Acknowledgements The work was funded by the Russian Science Foundation (Grant No. 25-69-00047, https://rscf.ru/project/25-69-00047/).

Data availability The data presented in this study are available on request from the corresponding author.

References

1. C.E. Myers, A. Interian, A.A. Moustafa, A practical introduction to using the drift diffusion model of decision-making in cognitive psychology, neuroscience, and health sciences. Front. Psychol. **13**, 1039172 (2022)
2. W. Pan, H. Geng, L. Zhang, A. Fengler, M.J. Frank, R.Y. Zhang et al., dockerHDDM: a user-friendly environment for Bayesian hierarchical drift–diffusion modeling. Adv. Methods Pract. Psychol. Sci. **8**(1), 25152459241298700 (2025)
3. P.M. Kraemer, S. Gluth, Episodic memory retrieval affects the onset and dynamics of evidence accumulation during value-based decisions. J. Cogn. Neurosci. **35**(4), 692–714 (2023)
4. X. Hu, C. Yang, L. Luo, Retrospective confidence rating about memory performance is affected by both retrieval fluency and non-decision time. Metacogn. Learn. **17**(2), 651–681 (2022)
5. J. Zou, Y. Qi, S. Tu, Y. Zhang, H. Zhao, J. Liu et al., The impact of smoking cues on working memory: evidence from the drift–diffusion model and EEG. Addict. Behav. **2025**, 108430 (2025)
6. M.K. van Vugt, M.A. Beulen, N.A. Taatgen, Relation between centro-parietal positivity and diffusion model parameters in both perceptual and memory-based decision making. Brain Res. **1715**, 1–12 (2019)
7. E. Bullmore, O. Sporns, Complex brain networks: graph theoretical analysis of structural and functional systems. Nat. Rev. Neurosci. **10**(3), 186–198 (2009)
8. A.E. Hramov, N.S. Frolov, V.A. Maksimenko, S.A. Kurkin, V.B. Kazantsev, A.N. Pisarchik, Functional networks of the brain: from connectivity restoration to dynamic integration. Phys. Usp. **64**(6), 584–616 (2021)
9. M. Perovnik, T. Rus, K.A. Schindlbeck, D. Eidelberg, Functional brain networks in the evaluation of patients with neurodegenerative disorders. Nat. Rev. Neurol. **19**(2), 73–90 (2023)
10. K. Erciyes, Complex brain networks: a graph-theoretical analysis. Bioinform. Brain **2024**, 224–249 (2024)
11. M. Rubinov, O. Sporns, Complex network measures of brain connectivity: uses and interpretations. Neuroimage **52**(3), 1059–1069 (2010)
12. P. Ranasinghe, M.S. Mapa, Functional connectivity and cognitive decline: a review of rs-fMRI, EEG, MEG, and graph theory approaches in aging and dementia. Explor. Med. **5**(6), 797–821 (2024)
13. V.V. Makarov, M.O. Zhuravlev, A.E. Runnova, P. Protasov, V.A. Maksimenko, N.S. Frolov et al., Betweenness centrality in multiplex brain network during mental task evaluation. Phys. Rev. E **98**(6), 062413 (2018)
14. V.A. Maksimenko, A.E. Runnova, N.S. Frolov, V.V. Makarov, V. Nedaivozov, A.A. Koronovskii et al., Multiscale neural connectivity during human sensory processing in the brain. Phys. Rev. E **97**(5), 052405 (2018)
15. P. Fransson, M. Strindberg, Brain network integration, segregation and quasi-periodic activation and deactivation during tasks and rest. Neuroimage **268**, 119890 (2023)
16. Y.M. Han, M.C. Chan, M.M. Chan, M.K. Yeung, A.S. Chan, Effects of working memory load on frontal connectivity in children with autism spectrum disorder: a fNIRS study. Sci. Rep. **12**(1), 1522 (2022)
17. O.E. Karpov, E.N. Pitsik, S.A. Kurkin, V.A. Maksimenko, A.V. Gusev, N.N. Shusharina et al., Analysis of publication activity and research trends in the field of AI medical applications: network approach. Int. J. Environ. Res. Public Health **20**, 5335 (2023). https://doi.org/10.3390/ijerph20075335
18. A.E. Hramov, V. Grubov, A. Badarin, V.A. Maksimenko, A.N. Pisarchik, Functional near-infrared spectroscopy for the classification of motor-related brain activity on the sensor-level. Sensors **20**, 2362 (2020). https://doi.org/10.3390/s20082362
19. V.V. Grubov, M.V. Khramova, S. Goman, A.A. Badarin, S.A. Kurkin, D.A. Andrikov et al., Open-loop neuroadaptive system for enhancing student's cognitive abilities in learning. IEEE Access **12**, 49034–49049 (2024). https://doi.org/10.1109/ACCESS.2024.3383847
20. A. Badarin, Riemannian geometry of eye-movement covariance matrices during a prolonged working memory task. Eur. Phys. J. Spec. Top. (2026). https://doi.org/10.1140/epjs/s11734-026-02366-z
21. P. Shepherdson, K. Oberauer, A.S. Souza, Working memory load and the retro-cue effect: a diffusion model account. J. Exp. Psychol. Hum. Percept. Perform. **44**(2), 286 (2018)
22. V. Khorev, A. Kiselev, A. Badarin, V. Antipov, O. Drapkina, S. Kurkin et al., Review on the use of AI-based methods and tools for treating mental conditions and mental rehabilitation. Eur. Phys. J. Spec. Top. **234**, 4139–4158 (2025). https://doi.org/10.1140/epjs/s11734-024-01289-x
23. V. Khorev, S. Kurkin, A. Badarin, V. Antipov, E. Pitsik, A. Andreev et al., Review on the use of brain computer interface rehabilitation methods for treating mental and neurological conditions. J. Integr. Neurosci. **23**(7), 125 (2024). https://doi.org/10.31083/j.jin2307125
24. S. Gordleeva, N. Grigorev, E. Pitsik, S. Kurkin, V. Kazantsev, A. Hramov, Detection and rehabilitation of age-related motor skills impairment: neurophysiological biomarkers and perspectives. Ageing Res. Rev. **2025**, 102923 (2025)
25. S. Sternberg, High-speed scanning in human memory. Science **153**(3736), 652–654 (1966)
26. S. Sternberg, Memory-scanning: mental processes revealed by reaction-time experiments. Am. Sci. **57**(4), 421–457 (1969)
27. A.A. Badarin, V.M. Antipov, V.V. Grubov, A.V. Andreev, E.N. Pitsik, S.A. Kurkin et al., Brain compensatory mechanisms during the prolonged cognitive task: fNIRS and eye-tracking study. IEEE Trans. Cogn. Develop. Syst. **17**(2), 303–314 (2024)
28. L. Kocsis, P. Herman, A. Eke, The modified beer-lambert law revisited. Phys. Med. Biol. **51**(5), N91–N98 (2006)
29. L. Duan, Y.J. Zhang, C.Z. Zhu, Quantitative comparison of resting-state functional connectivity derived from fNIRS and fMRI: a simultaneous recording study. Neuroimage **60**(4), 2008–2018 (2012)

30. M.W. Cole, S. Pathak, W. Schneider, Identifying the brain's most globally connected regions. Neuroimage **49**(4), 3132–3148 (2010)
31. J.P. Onnela, J. Saramäki, J. Kertész, K. Kaski, Intensity and coherence of motifs in weighted complex networks. Phys. Rev. E-Stat. Nonlinear Soft Matter Phys. **71**(6), 065103 (2005)
32. D. Bates, M. Mächler, B. Bolker, S. Walker, Fitting linear mixed-effects models using lme4. J. Stat. Softw. **67**, 1–48 (2015)
33. S. Lo, S. Andrews, To transform or not to transform: using generalized linear mixed models to analyse reaction time data. Front. Psychol. **6**, 1171 (2015)
34. H.D. Lucas, M.C. Duff, N.J. Cohen, The hippocampus promotes effective saccadic information gathering in humans. J. Cogn. Neurosci. **31**(2), 186–201 (2019)
35. S.C. Low, P.F. Verschure, D. Santos-Pata, Saccade rate is associated with recall of items in working memory. Learn. Mem. **29**(6), 146–154 (2022)

Springer Nature or its licensor (e.g. a society or other partner) holds exclusive rights to this article under a publishing agreement with the author(s) or other rightsholder(s); author self-archiving of the accepted manuscript version of this article is solely governed by the terms of such publishing agreement and applicable law.